

# MEASUREMENT OF SPATIAL DISPLACEMENT OF X-RAYS IN CRYSTALS FOR SELF-SEEDING APPLICATIONS

A. Rodriguez-Fernandez\*, B. F. Pedrini, S. Reiche, Paul Scherrer Institut, 5232 Villigen PSI, Switzerland

K. D. Finkelstein, CHESS, Cornell University, Ithaca, New York, USA

## Abstract

SASE Free-electron laser (FEL) radiation arises from shot noise in the electron bunch, which is amplified along the undulator section and results in X-ray pulses consisting of many longitudinal modes [1]. The output bandwidth of FELs can be decreased by seeding the FEL process with longitudinally coherent radiation. In the hard x-ray region, there are no suitable external seeding sources. Self-seeding represents a viable alternative. The X-ray beam is separated from the electrons using a magnetic chicane, and then monochromatized. The monochromatized X-rays serve as a narrowband seed, after recombination with the electron bunch, along the downstream undulators. This scheme generates longitudinally coherent FEL pulses.

Geloni et al. [2] have proposed monochromatization based on Forward Bragg Diffraction (FBD), which introduces a delay of the narrowband X-rays pulse of the order of femtoseconds that can be matched to the delay of the electron bunch due to the chicane. The FBD process produces a small transverse displacement of the X-ray beam, which may result in the loss of efficiency of the seeding process [3]. Preliminary results from an experiment performed at Cornell High Energy Synchrotron Source (CHESS) seem to confirm the predicted transverse displacement, which is therefore to be taken into account in the design of self-seeding infrastructure for optimizing the FEL performance.

## INTRODUCTION

X-ray free-electron lasers (FELs) relying on the self-amplified spontaneous emission (SASE) exhibit peak brightnesses many orders of magnitude larger than that from insertion devices at third-generation synchrotron sources [4,5]. The SASE radiation spectrum consists of many longitudinal modes, as a result of shot noise initiation of the amplification process in the electron beam [1,6]. For high-gain FELs, the normalized frequency bandwidth is  $\Delta\omega/\omega \sim \rho$ , where  $\rho$  is the FEL Pierce parameter [7]. At the future Swiss Free Electron Laser facility  $\rho = 4 \cdot 10^{-4}$ .

The bandwidth can be reduced by seeding the FEL with longitudinally coherent radiation coming from an external source. In the hard X-ray regime, where no external sources are available, a self-seeding scheme has been proposed by Geloni et al. [2]. This method exploits the time-domain features of the radiation transmitted in forward direction by a thin crystal in Bragg or Laue

diffraction geometry, called the “wake monochromator”. Unfortunately, the Forward Bragg Diffraction (FBD) process produces a small transverse displacement of the narrow-bandwidth, time-delayed X-ray seeding pulse, which results, if not compensated, in the loss of efficiency of the seeding process [3,8]. Until now the transverse displacement has not been studied experimentally. For a proper design of the seeding infrastructure, a quantitative understanding is mandatory, especially at the shorter wavelengths of 1 Å and below that will be offered at the Swiss Free Electron Laser (SwissFEL) facility.

With this contribution, we intend to present first results from an experimental study of the transverse displacement due to FBD. Our first experiment was performed at beamline C1 of the CHESS facility. These first results help to guide new experiments at FEL facilities. The present investigations will serve to validate or ameliorate our simulation tool. This will then be applied to calculate the propagation of the X-ray signal through the designed self-seeding unit of SwissFEL with the simulation software for FELs, GENESIS [9].

## THEORY OF TIME DEPENDENT X-RAY DYNAMICAL DIFFRACTION

Shvyd'ko et al. [3] present a series of analytic expressions resulting from a spatiotemporal system of wave equations which represent the shape and power of the monochromatic wave generated by an incident broad spectrum beam. In a previous work Lindberg et al. [8] presented how, from the coupled wave system of Bragg diffraction one can obtain solutions for both reflected and transmitted wave fields. They showed the relation between the resulting temporal profile and crystal properties, which include the x-ray extinction length  $\Lambda$ , the incident angle  $\theta$  for specific reflection, and in the case of the forward diffracted contribution, thickness  $d$  of the crystal. If the system of waves is solved for an incoming pulse beam it is possible to observe ‘echos’. The transverse displacement  $\Delta x_0$  is given by

$$\Delta x_0 = c \tau \cos(\theta), \quad (1)$$

where  $c$  is the speed of light and  $\tau$  denotes the time difference between the undiffracted beam and the ‘echo’ leaving the rear surface.

### *Spatiotemporal Dynamical Diffraction*

Lindberg and co-workers in Ref [8] derive an expression for the reflected and forward diffracted

\*angel.rodriguez@psi.ch

wavefields at the surface of the crystal as a function of  $A_0$  the initial incident wave. For the study of a wake monochromator crystal they obtain the following approximation to the outgoing wave

$$A_{0|P} = R_0 A_{0|Q} - \int_A^Q d\zeta' R_0(\zeta, \xi; \zeta', \zeta') \frac{ik_0 \chi_h}{2 \sin(\theta)} A_h - \int_A^Q d\zeta' A_0(\zeta', \zeta') \frac{\partial}{\partial \zeta'} R_0(\zeta, \xi; \zeta', \zeta') \Big|_{\xi=\zeta'} \quad (2)$$

Here,  $h$  denotes reciprocal lattice vectors inside the crystal that satisfy the diffraction condition. The amplitude  $R_0$  denotes the forward diffracted signal at the rear and front surfaces, respectively.  $R_0$  denotes the well-known Riemann function from the dynamical theory [3,8,10].  $k_0$  is the modulus of the x-ray wavevector inside/outside the crystal and  $\chi_h$  is  $h$ -Fourier component of crystal polarizability [10].

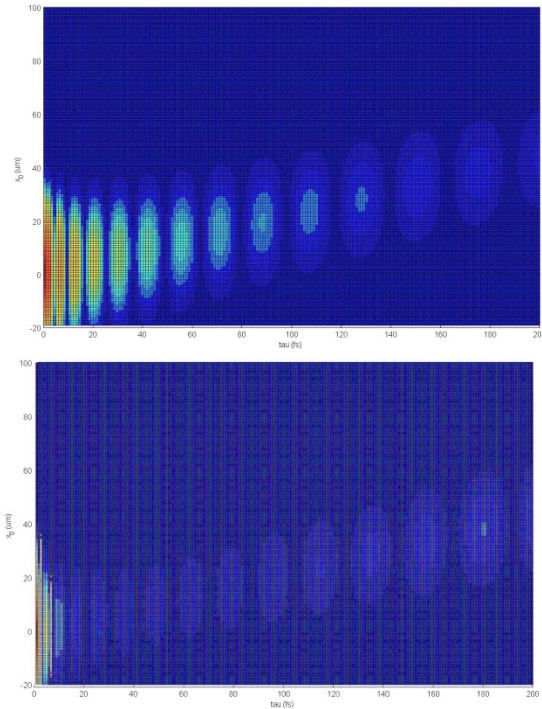


Figure 1: Forward diffracted field magnitude  $|E_h|$  from the (400) Bragg reflection at 10 keV for a 600  $\mu\text{m}$  thick Diamond crystal in the case of a 10  $\mu\text{m}$  size incident x-ray beam. (Above) Calculated following Lindberg and Shvyd'ko approximation for (3) and (below) calculated taking into account all the terms in (2).

In equation (2), the authors of [8] consider only the third term, which is relevant for time delays  $0 < c\tau < 2d/\sin(\theta)$ . With several assumptions, the obtained amplitude of the forward diffracted wavefield becomes

$$E_{0|P|3} = \frac{d\pi^2}{\Lambda^2 \sin(\theta)} e^{ik_0 \chi_h (d+c\tau/\sin(\theta))/2 \sin(\theta)} e^{-\frac{[x_0 - c\tau \cot(\theta)]^2}{4\sigma_x^2}} \times \frac{J_1 \left[ \pi \sqrt{c\tau} \left( 2d/\sin(\theta) + c\tau/\sin^2(\theta) \right) / \Lambda \right]}{\pi \sqrt{c\tau} \left( 2d/\sin(\theta) + c\tau/\sin^2(\theta) \right) / \Lambda} \quad (3)$$

where  $\sigma_x$  is the width of the incoming pulse in the transverse direction. For a 100  $\mu\text{m}$  thick diamond crystal at  $\theta = 44.04^\circ$ , the range of validity for the approximation is  $0 < c\tau < 300$  fs, and the first echoes are predicted to emerge at 10-20 fs delay relative to the undiffracted pulse.

In our first experiments taking place at synchrotron sources, the total pulse lengths was of the order of tens of picoseconds, and the signal from the forward diffracted beam results from integration over all positive time delays  $\tau = 0$ . Therefore, we must also take into account the first two terms neglected in equation (2). Using analog approximations as those used in Ref [8] for the third term, we calculated the corresponding two wave amplitudes of the forward diffracted beam and obtained

$$E_{0|P|1} = \frac{1}{4\pi \sin(\theta)} e^{ik_0 \chi_h (d+c\tau/\sin(\theta))/2 \sin(\theta)} e^{-\frac{[x_0 - c\tau \cot(\theta)]^2}{4\sigma_x^2}} \times \left\{ J_0 \left[ 2\pi \sqrt{\frac{c\tau}{2 \sin(\theta)}} \left( d + \frac{c\tau}{2 \sin(\theta)} \right) / \Lambda \right] + \frac{c\tau}{d 2 \sin(\theta) + c\tau} J_2 \left[ 2\pi \sqrt{\frac{c\tau}{2 \sin(\theta)}} \left( d + \frac{c\tau}{2 \sin(\theta)} \right) / \Lambda \right] \right\} \quad (4)$$

and

$$E_{0|P|2} = \frac{k_0^2 \chi_h \chi_h^-}{\sin^2(\theta)} e^{ik_0 \chi_h (d+c\tau/\sin(\theta))/2 \sin(\theta)} e^{-\frac{[x_0 - c\tau \cot(\theta)]^2}{4\sigma_x^2}} \times \left\{ J_0 \left[ 2\pi \sqrt{\frac{c\tau}{2 \sin(\theta)}} \left( d + \frac{c\tau}{2 \sin(\theta)} \right) / \Lambda \right] + \frac{c\tau}{d 2 \sin(\theta) + c\tau} J_2 \left[ 2\pi \sqrt{\frac{c\tau}{2 \sin(\theta)}} \left( d + \frac{c\tau}{2 \sin(\theta)} \right) / \Lambda \right] \right\} \times \frac{J_1[\pi(c\tau)/\Lambda]}{\pi(c\tau)/\Lambda} \quad (5)$$

Figure 1 shows the amplitude transmitted in forward direction as a function of transverse displacement and time delay, for a 600  $\mu\text{m}$  thick diamond crystal in symmetric (4,0,0) Bragg geometry, and assuming a 10 keV, 10  $\mu\text{m}$  wide x-ray beam. Figure 1a and 1b are obtained neglecting and considering (4,5), respectively. The dependence of the echo transverse displacement on the echo delay expressed in (1) is clearly visible in both panels. However, the figure also illustrates that the second term in (2) causes echoes at later times and correspondingly enhanced transverse displacement.

## EXPERIMENTAL SET-UP

The simulations presented in Fig. 1 correspond to conditions of experiments performed at beamline C1 at CHESS to study diamonds of different thicknesses (200 and 600  $\mu\text{m}$ ) using the (400) Bragg reflection. We plan to validate the obtained results and to extend the within a

second experiment which will take place at Material Science beamline at Swiss Light Source (SLS).

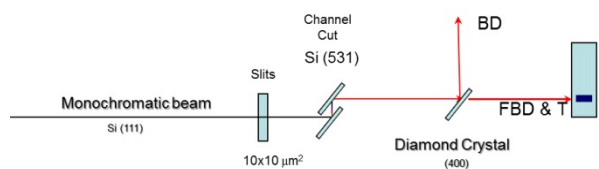


Figure 2: Experimental set-up for the experiment performed at C line at CHESS.

The beam characteristics required for the experiments (small energy bandwidth, beam size of about 10 μm and small angular divergence) are crucial. For this reason, after a Si (111) monochromator the beam is refined with a channel cut set of Si (531) crystals that reduce the angular width of incoming beam to 1.075°, which is slightly smaller than the expected Darwin acceptance for Diamond (400) Bragg reflection at 10 keV of 1.485°.

The layout of at the CHESS C-line is shown in Fig. 2. The beam size was set to 12±2 μm by slits located upstream the channel cut set of crystals. A NaI detector was situated in the Bragg diffraction direction, 44.04°, which mission was record the width and intensity of the Bragg diffracted signal. The detector in the forward direction uses a GGG scintillator crystal to convert x-ray to visible photons, which are recorded with an Andor camera with conventional resolution 6.5 μm/pixel after 10x magnification by means of an objective lens, leading to a resolution of 0.65μm/pixel. The sample under study was a diamond single crystal of 600 μm thickness. The crystal was set up to the maximum Bragg diffraction signal of the NaI detector at 10 keV, one fixed the channel cut set was rotated allowing just a determined energy to go through it with high resolution. Recording the signal transmitted thru the crystal in the Andor camera.

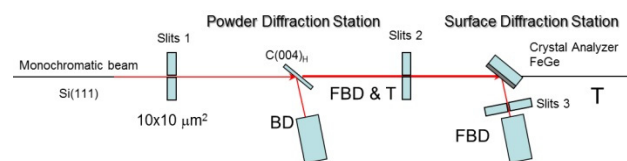


Figure 3: Experimental set-up at Material Science Beamline, SLS.

We have studied different diamond single crystals of thicknesses in the range 200 and 600 μmat the (400) reflection in symmetric Bragg geometry, and at 10 keV photon energy.

The foreseen setup for the future experiment at the SLS-MS beamline is shown Fig. 3. Beam divergence and size will be tuned with slits 0 and slits 1 in such a way to have parallel beam of 10 × 10 μm² size at the Powder Diffraction (PD) station. The crystals will be mounted at the center of the powder diffractometer on a high-

precision goniometer, and will be oriented appropriately by monitoring the Bragg Diffracted beam with the Mythen detector D1 placed on the PD diffractometer arm.

The transmitted beam, which includes the echoes generated from the FBD process, will proceed through the high-precision slits 2 located in the Surface Diffraction (SD) hutch. These will select transversally the portion of the beam impinging on the spectrometer, placed on the arm of the SD diffractometer. The spectrometer will consist of an analyzer crystal diffracting the beam through slits 3 onto a Pilatus detector D2. The X-ray spectra are acquired by rotating the analyzer crystal. This will be made of InSb, from which we do not expect any fluorescence signal, and which, in combination with a proper setting of slits 3, will fulfill the resolution requirements of better than the Darwin width of the diamond reflection under consideration.

We will first record reference spectra without crystal in the beam, at different transverse positions of slits 2. Then, the crystal will be mounted and oriented to be in perfect Bragg reflection geometry, determined by requiring the intensity of the Bragg diffracted beam on D1 to be maximal. At this point, a number of spectra will be recorded, again at different positions of slits 2. The procedure will be repeated at slightly different energies of the incoming beam, set with the Si(111) monochromator.

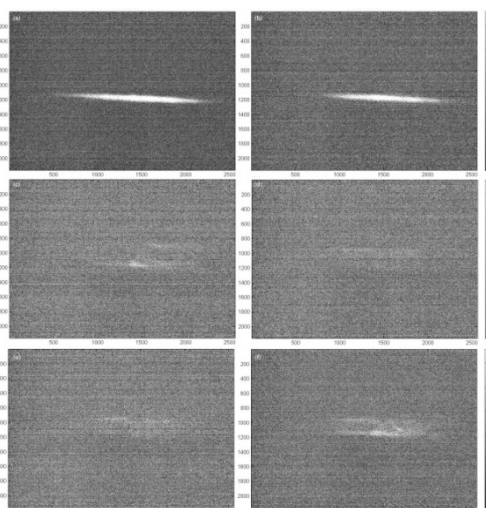


Figure 4: Forward Bragg Diffracted signal at six different energies for the 600 μm thick Diamond Crystal at the (400) reflection. (a) -2.50 eV, (b) -1.00 eV, (c) -0.87 eV, (d) 0 eV, (e) +0.03 eV and (f) +0.06 eV from 10 keV.

For this experiment we will be able to study five single crystal of diamond with different thicknesses 50, 100, 200, 500 and 600 μm. We also expect to be able to study the (400) reflection in the Bragg symmetry together with the Laue symmetry reflections (400), (220) and some asymmetric reflections as the (311).

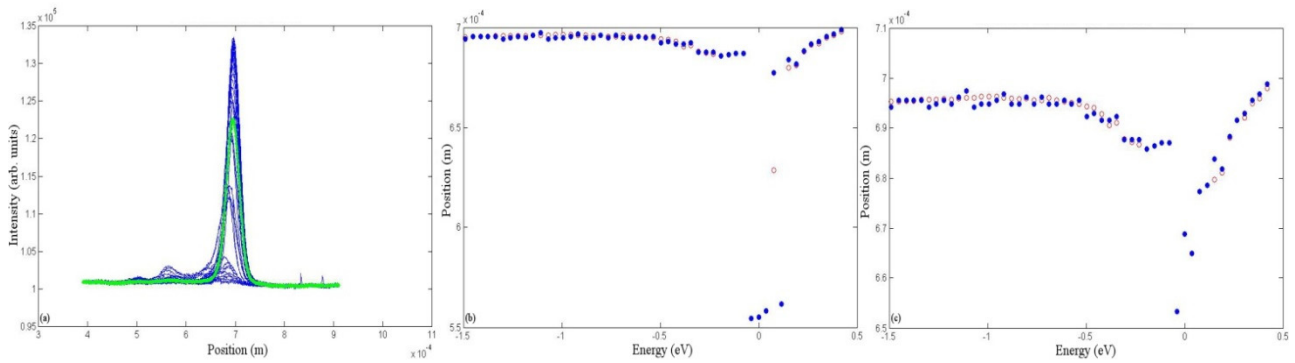


Figure 5: (a) Vertical cut of the forward diffracted signal recorder by the detector (Fig. 4) at different Energies near 10 keV. The reflection study was the symmetric (400) from a 600  $\mu\text{m}$  thick diamond, (b) Position of the Maximum peak for the different energies scan performed and (c) Position of the first maxima follow over the different energy scans. (Energy units are refer from the centre of the Bragg condition at 10 keV.

## FIRST RESULTS

In the experiment performed at C-line at CHESS, a 600  $\mu\text{m}$  thick diamond single crystal was studied for the (400) reflection at 10 keV,  $\theta = 44.04^\circ$ . As presented in Fig. 4, while rocking the channel cut set, keeping the diamond fixed to the maximum Bragg condition, we are able to perform energy scans that allow us to take pictures of the forward diffracted spatial distribution in  $x_0$  with high resolution.

It was observed how the intensity of the transmitted beam decreases considerably near the energy (10 keV) where the Bragg reflected beam intensity was maxima. This result tells us nearly all photons in the incident beam satisfied Bragg's law for the diamond 400 reflection. Since very few photons were "outside" the match to Bragg's law, the forward diffracted beam had a very small "contamination" from undiffracted radiation.

The vertical profile of the FWD signal, as presented in Fig. 5a, showed a decreasing of the transmitted intensity as a reduction of the area below the curve while approaching the Bragg condition as it is expected, due to the Bragg dispersion. What is interesting for our study is the displacement of the maxima, Fig. 5b, if the initial maxima (outside the Bragg condition) is follow, it is observed a displacement of 40  $\mu\text{m}$ , this displacement can be related to the calculation presented by Lindberg and Sdvyd'ko [3,8]. Although, we also observed a second main peak that is related to the second term in (2), this maximum is 120  $\mu\text{m}$  displace from the initial maxima position and in terms of intensity, near the Bragg condition, is even bigger than the initial maxima. Time speaking this maximum will appear at times much larger than 200 fs, so it should not be considered for self-seeding.

## CONCLUSIONS

The initial step in the study of the transverse displacement occurring in the FBD process has been performed in view of its future application for self-seeding at FELs. For a 600  $\mu\text{m}$  thick diamond single

crystal, a transverse displacement of the order of 40  $\mu\text{m}$  is observed as we expected from the calculations by Shvyd'ko and Lindberg [8]. The future experiment that will be performed at SLS, where different thickness diamonds will be study at different Bragg reflections (220), (400) and (311) for both Laue and Bragg geometries, will help to increase our knowledge about this process.

## ACKNOWLEDGMENT

We will like to acknowledge Cornell High Energy Synchrotron Source for the beamtime given for perform the study. CHESS is supported by the NSF & NIH/NIGMS via NSF award DMR-1332208 Also to Bruce Patterson, who helped us in the discussion for the developing of the experimental technique.

## REFERENCES

- [1] J. S. Wark and R. W. Lee, J. Apply. Crystallogr. 32, 692 (1999)
- [2] G. Geloni, V. Kocharyan and E. Saldin DESY report 10-053 (2010).
- [3] Y. Shvyd'ko and R. Lindberg Phys. Rev. ST Accel. Beams 15, 100702 (2012)
- [4] A. M. Kondratenko and E. L. Saldin, Part. Accel. 10, 207 (1980)
- [5] J. Als-Nielsen and D. McMorrow Elements of Modern X-ray Physics, John Wiley & Sons, Inc, New York, 2011 (second edition).
- [6] F. N. Chukhovskii and E. Foster, Acta Crystallogr. Sect. A 51, 668 (1995)
- [7] R. Bonifacio, C. Pellegrini, and L. M. Narducci, Opt. Commun. 50, 373 (1984)
- [8] R. R. Lindberg and Y. V. Shvyd'ko, Phys. Rev. ST Accel. Beams 15, 050706 (2012)
- [9] S. Reiche, Nuclear Instruments and Methods in Physics Research A 429, 243 (1999)
- [10] B. W. Batterman and H. Cole, Rev. of Modern Phys. 26, 681 (1964)